ELSEVIER

Chemical Engineering Journal 92 (2003) 15–26

Chemical Engineering Journal

www.elsevier.com/locate/cej

Influence of secondary flow on diffusion with heterogeneous reaction

Vidhya Balasubramanian, Girija Jayaraman*, S.R.K. Iyengar

Department of Mathematics, Indian Institute of Technology, Hauz Khas, New Delhi 110016, India

Received 19 November 2001; accepted 13 April 2002

Abstract

The concentration distribution in a Newtonian fluid for the secondary flow in a curved tube with bulk/wall reaction is obtained for a range of parameter values using an axially marching spectral finite difference scheme. The results predominantly illustrate that for fixed extent of secondary flows there is an improvement in the performance of the reactor as the effect of bulk and wall reaction mechanisms intensify in the system. For the same magnitude (moderate effects) of bulk and wall reaction mechanisms, there appears to be an increased conversion/performance in the homogeneous case. For small values of the reaction parameters, the improvement in the performance (3%) is more due to the wall reaction than bulk reaction. But, for moderate values of the non-dimensional reaction parameters (around 10), the enhanced performance (28%) is more due to the bulk reaction than wall reaction. As the effects of secondary flow dominate, there is an improvement in the performance of the reactor irrespective of the reactivity of the solute and the results agree with those of Mashelkar and Venkatasubramanian [AIChE J. 313 (1985) 440] for the case of non-absorbing walls. It is also observed that the approach of isoconcentration profile to the stream line pattern occurs at a lower value of the curvature parameter in the presence of wall reaction. The study is extended to examine the modifications in the tracer response measurements due to the power law rheology of the flowing fluid. The salient observation, irrespective of the reactivity of the solute, is that the performance of the reactor is improved in the case of pseudoplastic fluids compared to dilatant fluids. This improvement is further enhanced due to the presence of mild wall reaction.

Keywords: Wall absorption; Interface transfer; Curved tube; Secondary flows; Spectral method

1. Introduction

Gas–liquid reactions are of considerable importance in chemical industries. The typical processes include oxidation, hydrogenation, chlorination, sulphonation and gas purification by scrubbing. In petrochemical applications, biotechnology and waste water treatment plants, the bubble column reactors are utilized for improved selectivity. In electro-chemical industries, the effect of hydrodynamics on ion exchange membranes have been widely used. Standards of pollution control focus on the purification of reaction mixtures and also monitor optimum parameters for running a chemical reaction so as to obtain the ambient toxin concentrations, levels of pesticides or water pollutants that may jeoparadize occupational safety or health. In all the above cases, information is required regarding the effluent bulk average concentration.

Evans and Kenney [13] calculated empirically the rate of diffusion of nitrogen gas injected into flowing hydrogen gas under conditions in which the nitrogen gas can be exchanged by diffusion with a retentive layer of stagnant gas held in a porous solid structure. The significance of reversible adsorption of chemically active solutes on the flow boundary was observed experimentally by Clifford et al. [8], when studying the diffusion of hydrogen atoms in flowing nitrogen. Boddington and Clifford [6] emphasized the important effects of these exchange processes and discussed a number of boundary conditions at the flow boundary. Plumb and Ryan [24] determined experimentally the rate of diffusion of oxygen atoms in flowing helium using a modification of Taylor's dispersion theory [29] for the case of passive species injected into flowing solvent. It is known that the dispersion models, in fact, incorporate the radial and longitudinal mixing effects into a single effective axial dispersion coefficient and give some kind of cross-section averaged description of the reactor. In this direction, fully developed dispersion studies when the tracer is irreversibly absorbed at the outer boundary were taken up by Sankarasubramanian and Gill [27], Lungu and Moffat [20], Smith [28] and Barton [4]. A more general boundary condition incorporating the history dependence was taken up by Purnama [23], who calculated the fully developed dispersion coefficients. The details of concentration distribution of a solute in a fluid in laminar flow through a straight tubular reactor

---

* Corresponding author.

1385-8947/02/$ – see front matter © 2002 Elsevier Science B.V. All rights reserved.
PII: S1385-8947(02)00085-2

coated with a retentive layer was analysed by Shankar and Lenhoff [26].

The local mass transfer mechanisms are greatly affected by the complex flow patterns as in helical coils. Fluids flowing in curved tubes are subjected to centrifugal forces, which contribute to the generation of secondary flows. This additional complexity is being used in most of the process applications utilising helical coils. For example, helically coiled tubes are often used as efficient mixing devices and as cooling coils in refrigeration equipments and nuclear water reactors. The hydrodynamics of the flow of a Newtonian fluid in a mildly curved tube was first analysed by Dean [11,12], and since then an extensive review of the flow phenomena was reported [5,17]. However, there appears to be very few studies on the models incorporating mass transfer mechanisms accompanied by chemical reactions in coiled tubes.

Mashelkar and Venkatasubramanian [22] solved numerically the steady state mass transfer of a homogeneously reactive solute in a mildly coiled tubular reactor using Dean's profiles. Jayaraman et al. [19] were the first to analyse the fully developed dispersion in a mildly curved tube with absorbing walls, using a two phase model. Their results validated using the corresponding experimental results showed that the influence of secondary flow on dispersion was reduced if the tracer was very soluble in the wall. Following the solution methodology of Jayaraman et al. [19], the case of weak absorption mechanism occurring at the flow boundary of curved tubular reactors was analysed by Balasubramanian et al. [2]. The analysis revealed that the dispersion mechanism was enhanced on account of weak losses at the flow boundary and the dominant effect of secondary flows was to cause a significant drop in the corresponding straight tube dispersion coefficients. Balasubramanian et al. [3] observed that as the value of the wall absorption parameter increased, the dispersion coefficient became less susceptible to the increase in secondary flow effects.

The emphasis in the above mentioned studies was on the longitudinal dispersion. Through the changes in the dispersion coefficient and hence the average concentration, the combined effect of secondary flow and boundary absorption was studied. But, applications to the petroleum industry, waste water treatment plants, etc. require information regarding the bulk concentration details at various axial locations of the flow reactor. Further, in practice, especially in chromatographic experiments, it is most likely that a cup-mixing concentration instead of an area-average concentration is measured. For such applications, it is necessary to calculate the concentration profiles at various axial locations of the continuous flow reactors as well as the velocity weighted bulk average concentrations.

The non-linear rheological properties induce strong variation of the velocity profiles (flow distributions) compared to those observed for a Newtonian fluid and hence also have an impact on the mass transfer processes. Recent developments indicate that the study of non-Newtonian fluids is useful in a wide variety of industrial processes like industrial waste flow, process slurry operations, the manufacture of inks, pigments and paints, polymer and plastic synthesis/fabrication, etc. The modified conversions in the presence of homogeneous chemical reactions due to non-Newtonian characteristics in laminar tubular reactor was presented by Homsy and Strohman [15] and Mashelkar [21]. A comprehensive review of flow in curved tubes of non-Newtonian fluids has been cited in a number of articles [1,5]. In the case of mass transfer processes of homogeneously reactive solutes in power law fluids flowing through mildly coiled tubes, Mashelkar and Venkatasubramanian [22] solved numerically the equation of convection diffusion using the velocity profiles derived by Raju and Rathna [25]. The authors presented the detailed spatial concentration distributions and bulk mean concentration at the outlet.

The objective of the present study is to examine the steady state mass transfer at the reactive wall of a mildly curved tubular reactor through a detailed analysis of the concentration field using the axially marching spectral finite difference method. In Section 2, the mathematical model in terms of the governing equation is presented. Sections 3.1 and 3.2 give the velocity profiles for a Newtonian and a power law fluid, respectively. The inlet and the boundary conditions are discussed in Section 4. In Section 5, we analyse the Newtonian case using the spectral method of solution and the method of solution is extended for power law fluids using the velocity profiles derived by Raju and Rathna [25]. The bulk average concentration is computed in Section 6. The effect of interaction of the Dean number (N), bulk (α) and wall (β) reaction parameters on the mass transfer for the Newtonian case is studied in Section 7. The effect of power law index on the flowing fluid is examined in Section 7.1. A brief summary of the results is presented in Section 8. The results of the analysis are first verified in the case of straight tubular reactor and the results in the case of bulk reaction in a power law fluid flowing through a mildly curved tube are verified with [22]. Irrespective of the reactivity of the solute, an improved performance is observed in the case of pseudoplastic fluid compared to dilatant fluids. An improved reactor performance was found in the presence of mild wall reaction compared to the same magnitude of the bulk reaction parameter. However, the reactor performance was always better in the case of moderate to large reactions occurring in the bulk compared to the same magnitude of the reaction at the wall.

2. Mathematical formulation

The fluid dynamic behaviour in a circular curved tube of given curvature ratio, ($\lambda = b/a$, where b is the coil radius and a the tube radius) is characterized by the Dean number $N^{1/2} (= Re/\sqrt{\lambda})$ where Re is the Reynolds number based on the radius of the tube [11,12]. The toroidal coordinate system (r, θ, ϕ) for the simulation of the motion of the Newtonian

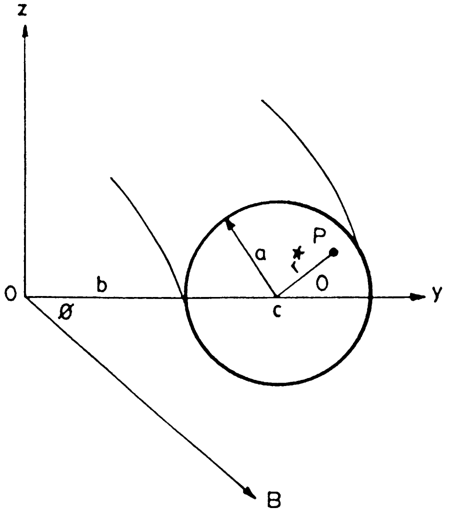

Fig. 1. Toroidal coordinate system.

fluid flowing through a circular tube of radius a, coiled in the form of a circle is illustrated in Fig. 1.

ZOC and BOC are the vertical and horizontal planes, respectively. OZ denotes the axis of the circle around which the tube is coiled. C represents the centre of cross-section of the tube in a plane which makes an angle ϕ with the fixed axial plane. OC is of length b, which is the radius of curvature of the coiled system, r^* denotes the distance CP and θ is the angle which CP makes with the line OC produced.

The steady state mass transfer of a homogeneously reactive solute of concentration c in a fully developed laminar flow of a Newtonian fluid flowing through a mildly coiled tube is considered. The convective diffusion equation, under the assumption that the influence of axial convection is much stronger than the axial molecular diffusion, is given by

$$\sigma\left[u\frac{\partial c}{\partial r}+\frac{v}{r}\frac{\partial c}{\partial \theta}\right]+w\frac{\partial c}{\partial z}=\frac{1}{r}\frac{\partial}{\partial r}\left[r\frac{\partial c}{\partial r}\right]+\frac{1}{r^2}\frac{\partial^2 c}{\partial \theta^2}-\alpha c \tag{1}$$

where c_R is a reference concentration, ν the kinematic viscosity, $Pe=(aw_m)/D_m$ the Péclét number, $\sigma=\nu/D_m$ the Schmidt number, w_m the mean axial velocity, D_m the molecular diffusivity, α the non-dimensional rate constant for a first order reaction. u^*, v^*, w^* represent the dimensional velocity components along the r, θ, ϕ directions, respectively, and the remaining starred variables represent the corresponding dimensional quantities.

3. Velocity profiles

For flow through tubes of small curvature, we use the first few terms of the Dean's/Raju and Rathna's expressions for the velocity field for Newtonian and power law models, respectively (the expressions being valid for moderately large values of N). The perturbation series expansions for the axial velocity component w and the stream function ψ are written as

$$w=w_0+Nw_1+N^2w_2+\cdots \tag{3}$$

$$\psi=Nf_1(r)\sin\theta+N^2f_2(r)\sin 2\theta+\cdots \tag{4}$$

where $w_1=w_{11}(r)\cos\theta$ and $w_2=w_{20}(r)+w_{20}^{\dagger}(r)\cos 2\theta$. The components of the secondary flow velocities, u, v are obtained from

$$u=\frac{1}{r}\frac{\partial\psi}{\partial\theta},\qquad v=-\frac{\partial\psi}{\partial r} \tag{5}$$

For the computation of the bulk average concentration we do not need the expressions for $f_2(r)$ and $w_{20}^{\dagger}(r)$.

3.1. Newtonian fluids

In the case of Newtonian fluids, we use the leading terms of the modified velocity profiles proposed by Dean [11,12]. The expressions for w_0, w_{11}, w_{20} and f_1 are given by

$$w_0=2-2r^2,\qquad w_{11}=\frac{19r-40r^3+30r^5-10r^7+r^9}{1440},$$

$$w_{20}=\frac{-4119+21\,280r^2-46\,340r^4+55\,440r^6-39\,830r^8+17\,584r^{10}-4620r^{12}+640r^{14}-35r^{16}}{350\times 576^2}\quad\text{and}$$

$$f_1(r)=\frac{4r-9r^3+6r^5-r^7}{72}$$

with the scaled parameters and variables taken as

$$c=\frac{c^*}{c_R},\qquad r=\frac{r^*}{a},\qquad z=\frac{z^*}{a^2w_m/\nu},$$

$$(u,v)=(u^*,v^*)\left(\frac{\nu}{a}\right),\qquad w=\frac{w^*}{w_m},$$

$$t=\frac{t^*}{a^2/D_m},\qquad \alpha=\frac{\alpha^*a^2}{D_m} \tag{2}$$

3.2. Power law fluids

In this case, we use the leading terms of the modified velocity profiles derived by Raju and Rathna [25] in terms of the power law index n_p. We have

$$w_0=\frac{3n_p+1}{n_p+1}[1-r^{1+1/n_p}] \tag{6}$$

$$w_{11} = r^{1/n_\mathrm{p}} \left\{ \frac{30A_\mathrm{p}(1 - r^{1+1/n_\mathrm{p}}) - 60B_\mathrm{p}(n_\mathrm{p}+1)^2(1 - r^{S+1/n_\mathrm{p}})}{[(n_\mathrm{p}S+1)(n_\mathrm{p}S+2+n_\mathrm{p})] + 5D_\mathrm{p}(1 - r^{3(1+1/n_\mathrm{p})}) - 3E_\mathrm{p}(1 - r^4(1+1/n_\mathrm{p})} \right\} \tag{7}$$

and

$$\begin{aligned} f_1(r) &= [A_\mathrm{p}r + B_\mathrm{p}r^\mathrm{S} + D_\mathrm{p}r^{(3n_\mathrm{p}+2)/n_\mathrm{p}} \\ &\quad - E_\mathrm{p}r^{(4n_\mathrm{p}+3)/n_\mathrm{p}}]\sin\theta \end{aligned} \tag{8}$$

where the expressions for $A_\mathrm{p}, \ldots, E_\mathrm{p}$ are given in Appendix A.

4. Boundary conditions

The heterogeneous reaction mechanism occurring at the wall of the tubular reactor is given by

$$\frac{\partial c}{\partial r} = -\beta c \quad \text{at } r = 1 \tag{9}$$

where $\beta = \beta^* a/D_\mathrm{m}$, represents the non-dimensional wall reaction parameter and β^*, the corresponding dimensional rate constant for a first order reaction. In addition, the regularity condition at $r = 0$ (so that we require a finite concentration at the centre of the tube) and the symmetry condition at $\theta = 0$ and $\theta = \pi$, respectively, are imposed. Thus we have

$$\frac{\partial c}{\partial \theta} = 0 \quad \text{at } \theta = 0 \quad \text{and} \quad \theta = \pi \tag{10}$$

At the inlet, it is assumed that the fluid with constant concentration enters the tube so that

$$c = 1 \quad \text{at } z = 0 \tag{11}$$

5. Spectral method

In this section, following Jayaraman et al. [19], the solution of Eq. (1) along with the associated set of inlet and boundary conditions is attempted by the spectral method of analysis.

It was observed by Jayaraman et al. [19], that at low Dean number a small change in axial velocity profile w occurs because of the curvature and this has little effect on the mass transfer mechanisms. Thus, the straight tube axial velocity profile ($w \approx w_0$) was found sufficient for the solution of the convective diffusion equation (1). The solution to Eq. (1) was formulated in terms of the Fourier cosine series as

$$c(r, \theta, z) = c_0(r, z) + c_1(r, z)\cos\theta + c_2(r, z)\cos 2\theta + \cdots \tag{12}$$

It is to be noted that the coefficients c_l, $l = 0, 1, 2, \ldots,$ are dependent on the parameters N, σ, α and β. We multiply Eq. (1) by $\cos(l\theta)$, after substituting in the equation the series expansions for w, u, v and c from Eqs. (3)–(5) and (12) and integrate from 0 to 2π. We obtain the following system of $L+1$ partial differential equations (with the series truncated after L terms):

$$\begin{aligned} w_0\frac{\partial c_0}{\partial z} &= -\frac{N\sigma}{2r}[c_1 f_1]' + c_0'' + \frac{1}{r}c_0' - \alpha c_0, \\ w_0\frac{\partial c_1}{\partial z} &= -\frac{N\sigma}{2r}[2c_0' f_1 + 2(c_2 f_1)' - c_2' f_1] + c_1'' + \frac{1}{r}c_1' \\ &\quad - \left(\alpha + \frac{1}{r^2}\right)c_1, \\ w_0 = \frac{\partial c_l}{\partial z} &= -\frac{N\sigma}{2r}[(l+1)(c_{l+1}f_1)' - (l-1)(c_{l-1}f_1)' \\ &\quad - l(c_{l+1}' - c_{l-1}')f_1] + c_l'' + \frac{1}{r}c_1' - \left(\alpha + \frac{l^2}{r^2}\right)c_l \end{aligned} \tag{13}$$

$l = 2, 3, \ldots, L$, where dash denotes differentiation with respect to the radial direction.

The inlet condition at $z = 0$ (Eq. (11)) gives

$$c_l = \begin{cases} 1, & l = 0 \\ 0, & l > 0 \end{cases} \tag{14}$$

The boundary conditions reduce to the following:

(a) First order wall absorption (Eq. (9))

$$\frac{\partial c_l}{\partial r} = -\beta c_l \quad \text{for } l = 0, 1, \ldots, L \quad \text{at } r = 1 \tag{15}$$

(b) The condition of finite concentration at the centre of the tube requires that all the coefficients $c_l(r, z)$ must remain finite at $r = 0$. Following Johnson and Kamm [18], Jayaraman et al. [19], the conditions valid at $r = 0$ can be obtained as

$$c_l = 0 \quad \text{for } l = 1, 2, \ldots, L \quad \text{at } r = 0 \tag{16}$$

$$\frac{\partial c_0}{\partial r} = 0 \quad \text{at } r = 0 \tag{17}$$

The symmetry condition (Eq. (10)) at $\theta = 0$ and $\theta = \pi$ is automatically satisfied.

Eq. (13) was solved by using a second order finite difference scheme which marches along the axial direction. The resulting block tridiagonal system of equations at each axial location was solved using a block tridiagonal system solver (Appendix B). The number (L) of spectral modes required to describe the concentration distribution c_L, was fixed such that the concentration of the highest spectral mode was at most 1% of c_0. For $N\sigma \le 2500$, L was taken as 10. For $N\sigma > 2500$, L was increased with $N\sigma$ up to a maximum of $L = 30$ for $N\sigma = 10^5$.

We have also extended the spectral method of analysis discussed earlier in this section, to incorporate the effect of pseudoplasticity on the steady state mass transfer of a reactive solute in a mildly curved tubular reactor. The method of solution is on the same lines as that of the Newtonian fluids except that now the modified velocity profiles are used.

6. Bulk average concentration

The concentration (c) profile obtained by the spectral model was used to calculate the bulk average concentration at fixed axial locations. The bulk average concentration $c_{\mathrm{avg}}(z)$ using the spectral model is given by

$$c_{\mathrm{avg}}(z) = \frac{\int_0^{2\pi}\int_0^1 rwc\,\mathrm{d}r\,\mathrm{d}\theta}{\int_0^{2\pi}\int_0^1 rw\,\mathrm{d}r\,\mathrm{d}\theta} \qquad (18)$$

Substituting the expansions for w (Eq. (3)) and c (Eq. (12)) we have

$$c_{\mathrm{avg}}(z) = \frac{\int_0^{2\pi}\int_0^1 r[w_0 + Nw_1 + N^2w_2 + \cdots][c_0 + c_1\cos\theta + c_2\cos(2\theta) + \cdots]\,\mathrm{d}r\,\mathrm{d}\theta}{\int_0^{2\pi}\int_0^1 r[w_0 + Nw_1 + N^2w_2 + \cdots]\,\mathrm{d}r\,\mathrm{d}\theta} \qquad (19)$$

Simplifying we have the approximation

$$c_{\mathrm{avg}}(z) = \frac{\int_0^1 r[w_0c_0 + (Nw_{11}c_1/2) + N^2w_{20}c_0]\,\mathrm{d}r}{\int_0^1 r[w_0 + N_2w_{20}]\,\mathrm{d}r} \qquad (20)$$

The integrals in Eq. (20) were evaluated by using the Simpson rule.

7. Results and discussions

The steady state mass transfer of a reactive solute in a Newtonian fluid flowing through a mildly curved tubular reactor was analysed using the axially marching spectral finite difference technique. The cumulative effect on the reactor performance due to secondary flows along with the bulk (α) and wall (β) reaction parameters are examined. The reduction in the value of $\tilde{\xi}$ (reactor length) to achieve a fixed level of conversion $[1 - c_{\mathrm{avg}}(\tilde{\xi})]$ where $\tilde{\xi} = z/\sigma$ is considered as a measurement of the improved performance of the reactor. The admissible values [7,14,22] of the bulk reaction (α) and the wall reaction (β) parameters are taken as $\alpha = 0, 2, 6, 10$, and $\beta = 0, 2, 6, 10$, respectively. The overall performance on account of secondary flows was analysed in terms of the grouped parameter $N\sigma$ which is given the values of 2500, 5000 and 10 000. The group $N\sigma$ is the ratio of terms in the concentration equation representing convection by secondary motion to the diffusive terms and can be referred to as secondary flow Péclét number. When $N\sigma$ is large, then it means that σ is large since Dean's velocity profiles are used. The values of $N\sigma$ are taken as $N\sigma \geq 2500$ because smaller values do not yield significant deviations from the straight tube results. In the present analysis, the Schmidt number (σ) is taken of the order of 1000 and this is true for most liquids.

The effect of secondary flows along with the bulk (α) and wall (β) reaction parameters for a Newtonian fluid on the bulk average concentration at $\tilde{\xi} = 0.15$ is given in Table 1.

Table 1
Values of c_{avg} at $\tilde{\xi} = 0.15$ for a Newtonian fluid

α	β	$N\sigma = 0$	$N\sigma = 2500$	$N\sigma = 5000$	$N\sigma = 10\,000$
0	0	1.0	1.0	1.0	1.0
–	2	0.7114	0.6851	0.6746	0.6666
–	6	0.5836	0.5186	0.4919	0.4695
–	10	0.5454	0.4644	0.4313	0.4027
0	0	1.0	1.0	1.0	1.0
2	–	0.7483	0.7469	0.7465	0.7464
6	–	0.4357	0.4255	0.4226	0.4213
10	–	0.2645	0.2484	0.2438	0.2415
2	6	0.4700	0.4091	0.3855	0.3662
6	2	0.3519	0.3196	0.3086	0.3012

The accuracy of the solution obtained from the spectral method was first checked by comparing the bulk average concentration with the published results in the limiting case of the straight tubular reactors. For the case of solutes undergoing only the bulk reaction in a Newtonian fluid flowing through straight tubular reactors, the results are found to be in exact agreement with Cleland and Wilhelm [7] and Hsu [16].

We observe from Table 1 that as $N\sigma$ increases, i.e. as the effect of secondary flow dominates, there is an improvement in the performance of the reactor irrespective of the reactivity of the solute and the results are in agreement with those of Mashelkar and Venkatasubramanian [22] for the case of non-absorbing walls.

The performance of the straight and curved tubular reactors is influenced by the hydrodynamics of the fluid flow in these reactors. In straight tubular reactor, in the absence of any wall reaction, the elements near the wall which have low velocities undergo less homogeneous reaction. This situation is reversed for elements near the central core. Also, the only mechanism by which elements move across the radial direction is by molecular diffusion, which is an extremely slow process. However, in the case of coiled tubes, because of the secondary flows, the elements near the central core are brought to the outer wall and those near the outer wall are taken to the central core. This process helps in smoothing out the residence time distribution of the various elements, which is also a cause for the observed improved conversion.

Fig. 2 gives the effect of the wall reaction parameter on the bulk average concentration for a Newtonian fluid. Results from Table 1 and Fig. 2 indicate that for the same magnitude of bulk and wall reaction mechanisms, there appears to be an increased conversion/performance in the homogeneous case $\beta = 0$. For moderate values of the non-dimensional reaction parameters (around 10), the enhanced performance (28%) is more due to the bulk reaction than wall reaction. In

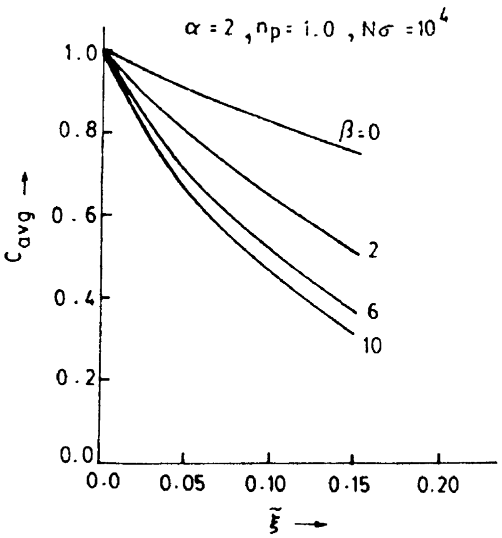

Fig. 2. Variation of the bulk average concentration c_{avg} with $\tilde{\xi}$ for values of β.

the case of a homogeneously reactive solute, the residence time of the various elements depends on the flow pattern of the flowing fluid. The residence time of various elements is increased on account of secondary flows as the flow becomes less effective in spreading the material longitudinally which results in the improved reactivity in the bulk. However, in the presence of a reactive wall, the elements around the wall area undergo reaction immediately on contact, whereas those at the centre are less affected resulting in a higher value of the bulk average concentration or a decreased performance (see Table 1). The presence of significant secondary flows in the system (within Dean constraint) tries to uniform out these differences which can only slightly increase the residence time of the various elements indicating an improvement in the performance on account of secondary flows in this case. In comparison to the case of bulk reaction, the extent of improvement in the performance of the reactor on account of secondary flows was found to be more significant when boundary reaction was also included.

The whole scenario is changed when we consider very mild effects of bulk or wall reaction mechanisms, say $\alpha \approx 2$ or $\beta \approx 2$ (Fig. 3a and b). An improved performance is observed because of the boundary reaction, i.e. for small values of the reaction parameters, the improvement in the performance (3%) is more due to the reaction at the wall than bulk reaction. As the rate of contaminant depletion at the wall is proportional to the wall absorption parameter β and the value of the concentration at the wall, we observe that for small β, a reduced c_{avg} is obtained. The secondary flow effect, in addition, further increases the residence time of the various elements thereby resulting in the much improved performance. However, as bulk reaction effects intensify in the system it is observed that the effect of wall reaction becomes less significant.

Fig. 4(i)–(vi) shows the isoconcentration profiles in Newtonian fluids for $\alpha = 2$ and for various values of β, $N\sigma$ at $\tilde{\xi} = 0.15$. β is fixed at 2 for (i)–(iii) and it varies from 0 to 6 in (iv)–(vi). For fixed extents of bulk (α) and wall (β) reaction effects, results indicate that the influence of secondary flow increases with the increase in the value of $N\sigma$. The secondary flow becomes more skewed towards the outer wall of the tube and at a particular value of $N\sigma$ say around 10^4, the concentration profile appears in two cell patterns. As $N\sigma$ is further increased, the increase in the intensity of secondary flows makes the concentration profile line up with the secondary flow streamlines. Further, it is observed that with boundary reaction, the approach of isoconcentration profile to the secondary flow stream line pattern occurs at a lower value of the $N\sigma$ (Fig. 4(iii) and (vi)). This is because of development of radial concentration gradients due to which the alignment of solute particles along the secondary flow streamline pattern occurs for a lower value of $N\sigma$ whereas in the presence of boundary reaction, the approach to streamline pattern is

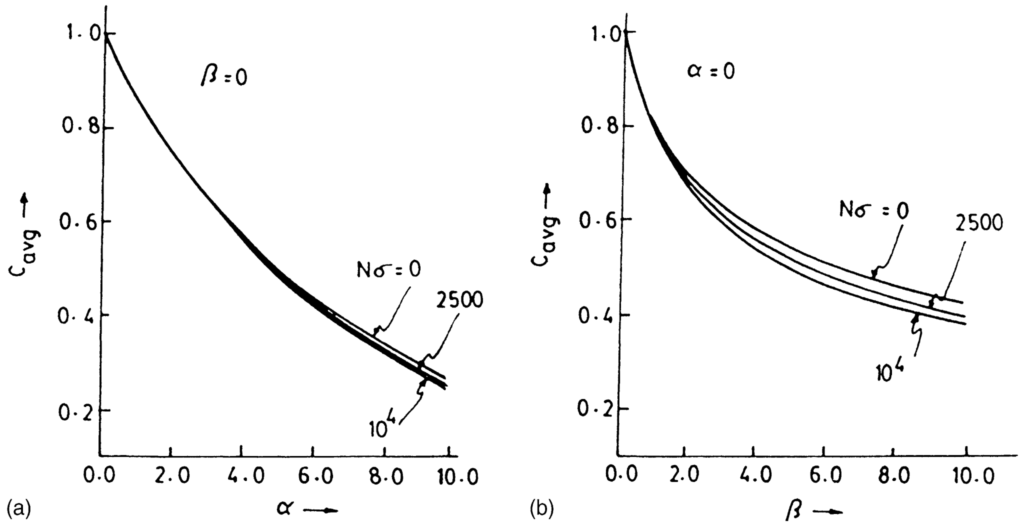

Fig. 3. Bulk average concentration c_{avg} in the case of Newtonian fluids at $\tilde{\xi} = 0.15$ for (a) $\beta = 0$ and (b) $\alpha = 0$.

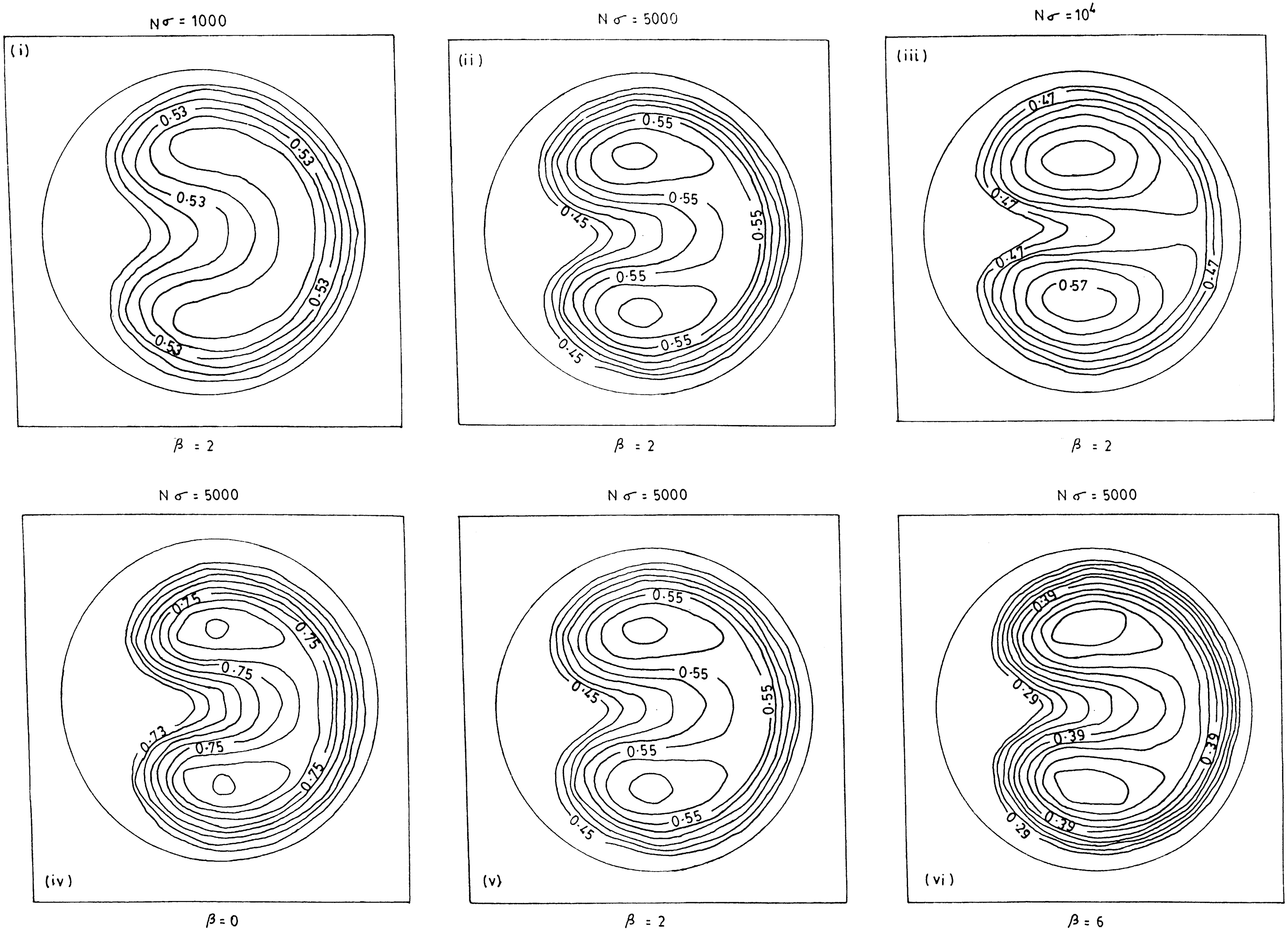

Fig. 4. (i)–(iii) Isoconcentration profiles at $\bar{\xi} = 0.15$ for $\alpha = 2$ and $\beta = 2$ in a Newtonian fluid; (iv)–(vi) isoconcentration profiles at $\bar{\xi} = 0.15$ for $\alpha = 2$ and $N\sigma = 5000$ and $\beta = 0, 2, 6$.

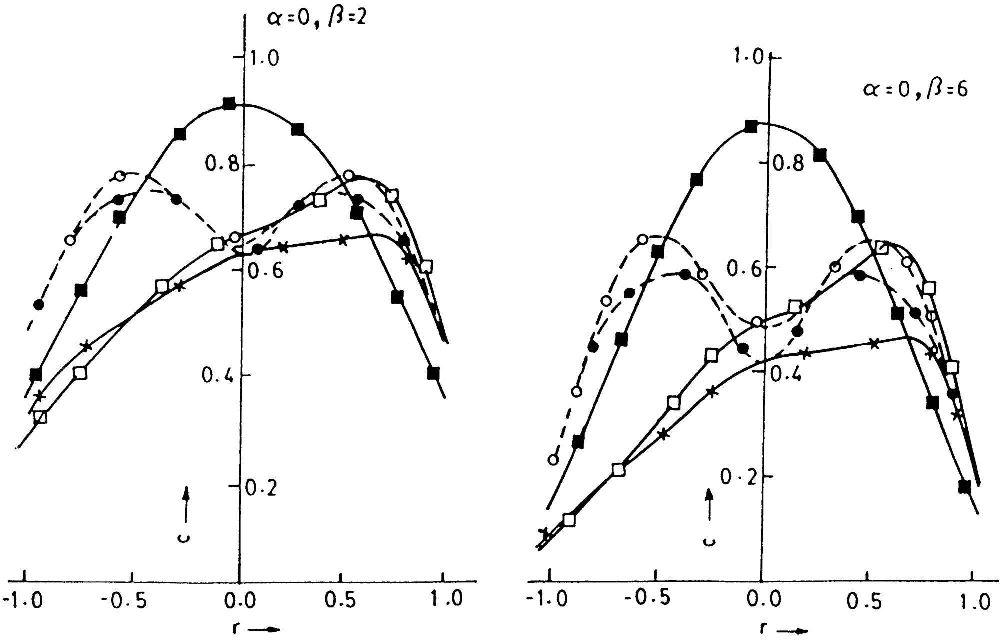

(a) (b)

Fig. 5. Local concentration profiles for a Newtonian fluid on the horizontal (c_H) and the vertical (c_V) planes at $\tilde{\xi} = 0.15$ and $N\sigma = 5000$ for: (a) $\alpha = 0$, $\beta = 2$; (b) $\alpha = 0$, $\beta = 6$. ○: c_V for $N\sigma = 2500$; □: c_H for $N\sigma = 2500$, ●: c_V for $N\sigma = 10\,000$, ×: c_H for $N\sigma = 10\,000$, ■: c_V for $N\sigma = 0$.

Table 2
Various order modifications in c_{avg} at $\tilde{\xi} = 0.15$ for $\alpha = 2$ and $\beta = 0$

$N\sigma$	c_{avg}	O(N)	O(N^2)
0	0.7483	0.0	0.0
1000	0.7480	0.2426×10^{-4}	0.1478×10^{-5}
2500	0.7469	0.1330×10^{-4}	0.1493×10^{-5}
3500	0.7465	0.9605×10^{-5}	0.1492×10^{-5}
5000	0.7984	0.7684×10^{-5}	0.1496×10^{-5}
10000	0.7464	0.4159×10^{-5}	0.1500×10^{-5}

in accordance with the flow details of the fluid. Once again, it is observed that as the bulk reaction effects increase, the effect of wall reaction becomes less significant.

Fig. 5a and b gives the variation of local concentration profiles on the horizontal (c_H) and vertical (c_V) planes of the coiled tubular reactor for the various values of the wall reaction parameters at $\tilde{\xi} = 0.15$. In view of the symmetric conditions with respect to θ (Eq. (10)) we find that the concentration profiles on the vertical plane (c_V) are symmetric. Because of the variation in the fluid motion towards the inner and the outer walls of the coiled tube, as in [22], the profiles on the horizontal (c_H) plane are non-symmetric. It can be further observed that when the solute undergoes boundary reaction, the ratio of maximum to minimum value of the point concentration in straight tubular reactor is more than that in a coiled tubular reactor. This is because, in comparison to the concentration profile in a straight tubular reactor, the profile is more uniform in a coiled tubular reactor.

Table 3
Various order modifications in c_{avg} at $\tilde{\xi} = 0.15$ for $\alpha = 0$ and $\beta = 2$

$N\sigma$	c_{avg}	O(N)	O(N^2)
0	0.7114	0.0	0.0
1000	0.7044	0.7636×10^{-4}	0.1492×10^{-5}
2500	0.6851	0.4220×10^{-4}	0.1550×10^{-5}
3500	0.6790	0.3217×10^{-4}	0.1551×10^{-5}
5000	0.6746	0.2699×10^{-4}	0.1568×10^{-5}
10000	0.6666	0.1512×10^{-4}	0.1588×10^{-5}

The bulk average concentration given by expression in Eq. (20) was further simplified to analyse (in Tables 2

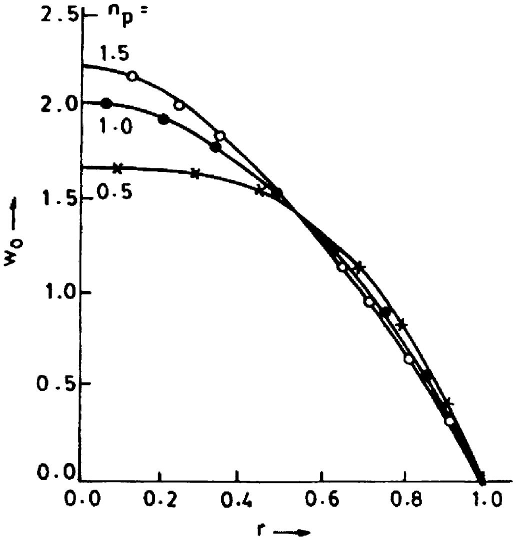

Fig. 6. Velocity profiles for a power law fluid.

and 3) the contribution due to the O(N) and O(N^2) terms of the axial velocity (w) profile. The terms are given by

$$c_{\mathrm{avg}}(z)\left[\int_0^1 rw_0\,\mathrm{d}r\right] = \int_0^1 rw_0c_0\,\mathrm{d}r + \frac{N}{2}\int_0^1 rw_{11}c_1\,\mathrm{d}r + N^2\left[\int_0^1 rw_{20}c_0\,\mathrm{d}r - \frac{\int_0^1 rw_0c_0\,\mathrm{d}r\int_0^1 rw_{20}\,\mathrm{d}r}{\int_0^1 rw_0\,\mathrm{d}r}\right] + \cdots \quad (21)$$

It is observed that the contribution of the O(N^2) terms are less significant compared to the contribution of the O(N) terms.

7.1. Extension to power law fluids

In this section, we extend our earlier discussion to the case when the fluid is represented by a power law model. The modified velocity profiles proposed by Raju and Rathna [25], in conjunction with the spectral method of solution was used to examine the effect of power law index (n_p) on the various tracer response measurements. The values of n_p

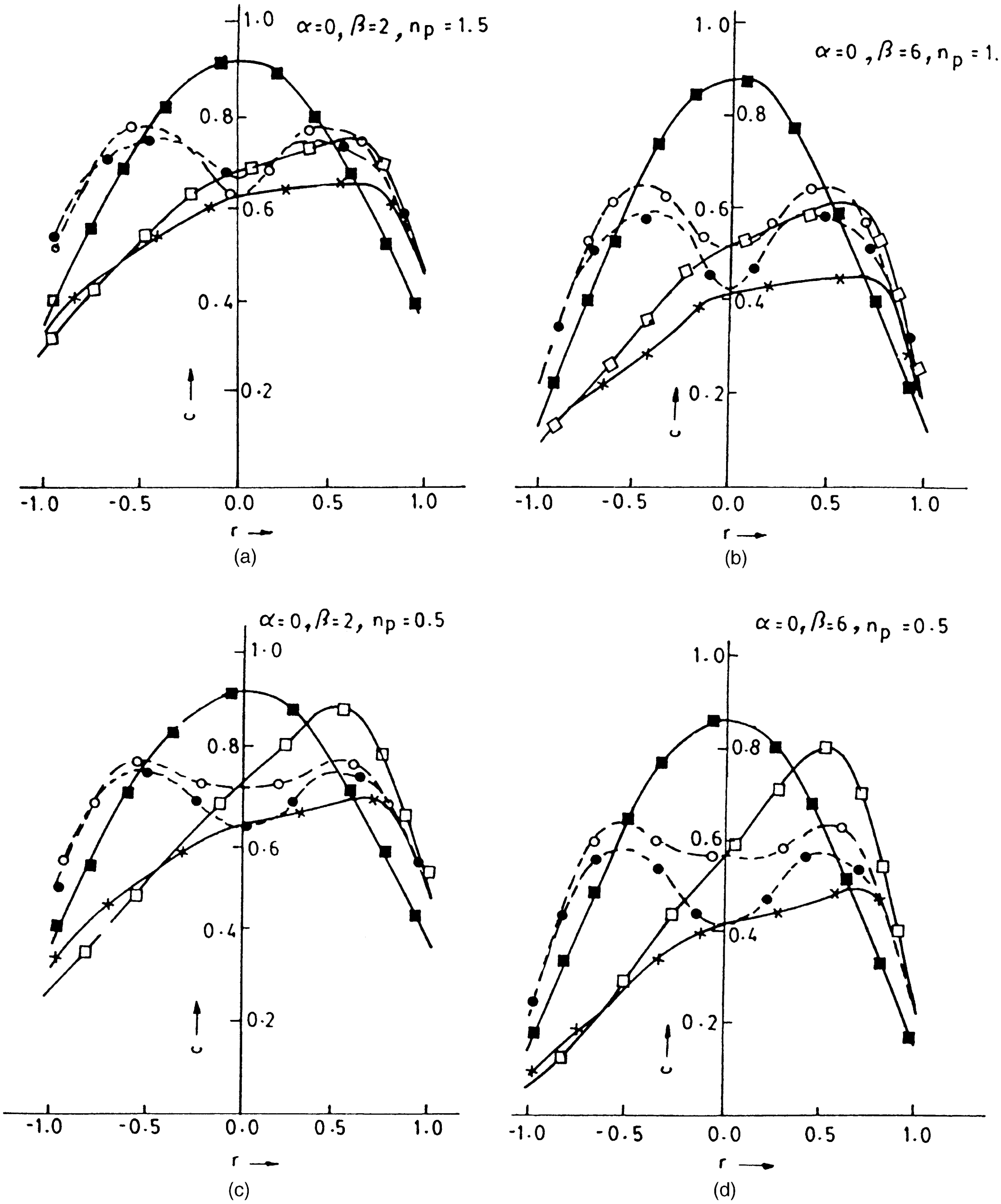

Fig. 7. Local concentration profiles on the horizontal (c_H) and the vertical (c_V) planes at $\tilde{\xi}=0.15$ and $N\sigma=5000$ for: (a) $\alpha=0$, $\beta=2$, $n_p=0.5$; (b) $\alpha=0$, $\beta=6$, $n_p=0.5$; (c) $\alpha=0$, $\beta=2$, $n_p=1.5$; (d) $\alpha=0$, $\beta=6$, $n_p=1.5$. ○: c_V for $N\sigma=2500$, □: c_H for $N\sigma=2500$, •: c_V for $N\sigma=10\,000$ ×: c_H for $N\sigma=10\,000$, ■: c_V for $N\sigma=0$.

Table 4
Influence of β, $N\sigma$ and n_p on c_{avg} at $\tilde{\xi} = 0.15$ for $\alpha = 0$

β	$N\sigma$	$n_p = 0.50$	$n_p = 0.75$	$n_p = 1.00$	$n_p = 1.25$	$n_p = 1.50$
2	0	0.7042	0.7088	0.7114	0.7132	0.7144
–	1000	0.7013	0.7035	0.7044	0.7050	0.7054
–	2500	0.6795	0.6841	0.6851	0.6853	0.6858
–	3500	0.6726	0.6780	0.6800	0.6803	0.6812
–	5000	0.6713	0.6729	0.6746	0.6756	0.6764
–	10000	0.6621	0.6651	0.6666	0.6672	0.6673
6	0	0.5678	0.5778	0.5836	0.5874	0.5901
–	1000	0.5607	0.5647	0.5657	0.5667	0.5671
–	2500	0.5307	0.5212	0.5186	0.5190	0.5201
–	3500	0.5081	0.5015	0.5030	0.5068	0.5087
–	5000	0.4849	0.4889	0.4919	0.4934	0.4956
–	10000	0.4600	0.4662	0.4695	0.4711	0.4718

are taken as 0.5, 0.75, 1.0, 1.25 and 1.50. Fig. 6 gives the variation of the velocity profile w_0 with r. In comparison to the velocity profiles for the Newtonian case, the profiles in the case of pseudoplastic ($n_p < 1$) fluids are blunt and those in case of dilatant ($n_p > 1$) fluids are sharper.

Fig. 7a–d gives the variation of local concentration profiles on the horizontal (c_H) and vertical (c_V) planes of the coiled tubular reactor for various values of the wall absorption parameter at $\tilde{\xi} = 0.15$. On the vertical plane (c_V), the local concentration decreases towards the inner wall and increases towards the outer wall as the power law index n_p decreases. Hence, in view of the nature of the velocity profiles of the pseudoplastic fluids, the ratio of maximum to minimum value of the point concentration was found to be less than that for a Newtonian fluid. It is also observed that the difference between the maximum and minimum value of the point concentration is more due to the reaction at the surface of the tube compared to the same magnitude of the bulk reaction parameter. Also, irrespective of the reaction mechanism it is observed from Fig. 7a–d that in the presence of mild secondary flows, the flattening effect of pseudoplastic fluid dominates. The two centres of counter rotating vortices appear at a lower value of $N\sigma$ for a dilatant fluid and in the presence of boundary reaction this value is further lowered.

When the effect of power law index (n_p) on the mass transfer processes of homogeneously reactive solute in straight tubular flow was taken into consideration, the results were found to agree with Mashelkar [21]. In comparison to the Newtonian case, it was observed that there was an improved conversion in both straight and curved tubular reactors [22] because of the pseudoplastic nature of the fluid. The effect of secondary flows along with the bulk and wall reaction mechanisms on the bulk average concentration at $\tilde{\xi} = 0.15$ is given in Table 4. Results indicate that irrespective of the pseudoplastic or dilatant nature of the fluid, the overall behaviour of the reactor on account of secondary flows and either one of the reaction parameters remain the same as that for the Newtonian case. It was found that in straight tubular reactors, the effect of increasing pseudoplasticity (reduced n_p) is to decrease the concentration of the reactant at any axial position and this helps in increasing the residence time of various elements in comparison to the Newtonian case. Hence, compared to the case of Newtonian fluids, a decreased value of the bulk average concentration or improved performance at any axial position is observed in case of pseudoplastic fluids. This improvement is further enhanced due to the presence of mild wall reaction.

The curvature effect on the isoconcentration profiles of the power law fluids is similar to that for the Newtonian fluid. For a fixed extent of reaction parameters, results indicate that with the increasing pseudoplasticity (reduced n_p) of the fluid, the intensity of secondary flow in power law fluid decreases whereas vice versa holds for a dilatant fluid. In addition, compared to the Newtonian fluids, the overall approach of the isoconcentration curves to the streamline patterns were observed to occur at a larger value of the curvature parameter $N\sigma$ for a pseudoplastic fluid and at a lower value of $N\sigma$ for a dilatant fluid. In each of these cases the value of the curvature parameter is further lowered due to mild reaction at the surface of the tube.

8. Conclusions

The evolution of the concentration distribution in a Newtonian fluid, over a range of parameter values for the secondary flow and bulk/wall reaction was obtained using an axially marching spectral finite difference scheme. The accuracy of the solution was first checked by obtaining the bulk average concentration in the limiting case of a laminar straight tubular reactor. Results predominantly illustrate that for fixed extent of secondary flows there was an improvement in the performance of the reactor as the effect of bulk and wall reaction mechanisms intensify in the system. For the same magnitude (moderate effects) of bulk and wall reaction mechanisms, there appears to be an increased conversion/performance in the homogeneous case. However, for small values of the reaction parameters there appears to be an improved performance because of wall reaction. As the effect of secondary flows dominate, there is an improvement in the performance of the reactor irrespective of the reactivity of the solute and the results are in agreement with those of Mashelkar and Venkatasubramanian [22] for the case of non-absorbing walls. It was also observed that the approach of isoconcentration profile to the stream line pattern occurred at a lower value of the curvature parameter due to the reaction at the surface of the tube.

This study was extended to examine the modifications in the tracer response measurements due to the power law rheology of the flowing fluid. The overall behaviour of the reactor in the case of power law fluids was found to be the same as that for the Newtonian case. The salient observation irrespective of the reactivity of the solute includes an improved performance of the reactor in case of pseudoplastic fluids compared to dilatant fluids. This improvement is further enhanced due to the presence of mild boundary reaction. In the presence of moderate to large effects of secondary flows, the overall approach of the isoconcentration curves to the streamline patterns were observed to occur at a larger value of the curvature parameter in the case of pseudoplastic fluids and at a lower value of the curvature parameter for a dilatant fluid. The value of the curvature parameter is further lowered due to mild reaction at the surface of the tube. This study is based on Dean's solution and hence the Dean number cannot take very large values. Corresponding to this solution, there is a single secondary flow vortex in each half of the tube. However, there is a critical value of the Dean number above which more than one steady solution exists [9] and these solutions are four vortex in character. This will affect the concentration profile as well and hence our results have to be modified significantly for large values of the Dean number.

The present study, with suitable modifications, can be applied for modelling of cross-flow microfiltration and the development of technique for overcoming the detrimental effects of membrane fouling [10].

Acknowledgements

The first author is thankful to the National Board for Higher Mathematics for the research assistantship. The authors are grateful to the referees for the suggestions which have greatly improved the contents of the manuscript.

Appendix A

$$S = \frac{(n_\mathrm{p}+1)+\sqrt{17n_\mathrm{p}^2-2n_\mathrm{p}+1}}{2n_\mathrm{p}},$$

$$A_\mathrm{p}^1 = n_\mathrm{p}S[21n_\mathrm{p}^3+53n_\mathrm{p}^2+38n_\mathrm{p}+8],$$

$$A_\mathrm{p}^2 = 60n_\mathrm{p}^4+185n_\mathrm{p}^3+200n_\mathrm{p}^2+92n_\mathrm{p}+15,$$

$$A_\mathrm{p}^3 = 12(n_\mathrm{p}+1)(1-S)(2n_\mathrm{p}+1)(3n_\mathrm{p}+1),$$

$$A_\mathrm{p}^4 = (4n_\mathrm{p}^2+9n_\mathrm{p}+3)(n_\mathrm{p}^2+4n_\mathrm{p}+1),$$

$$A_\mathrm{p} = \frac{n_\mathrm{p}^3(n_\mathrm{p}SA_\mathrm{p}^1-A_\mathrm{p}^2)}{A_\mathrm{p}^3A_\mathrm{p}^4},$$

$$B_\mathrm{p}^1 = 4(1-S)(2n_\mathrm{p}+1)(3n_\mathrm{p}+1)A_\mathrm{p}^4,$$

$$B_\mathrm{p} = \frac{n_\mathrm{p}^3(13n_\mathrm{p}^3+31n_\mathrm{p}^2+23n_\mathrm{p}+5)}{B_\mathrm{p}^1},$$

$$D_\mathrm{p} = \frac{n_\mathrm{p}^4}{4(1+n_\mathrm{p})(3n_\mathrm{p}+1)(n_\mathrm{p}^2+4n_\mathrm{p}+1)},$$

$$E_\mathrm{p} = \frac{n_\mathrm{p}^4}{12(n_\mathrm{p}+1)(3n_\mathrm{p}+1)(4n_\mathrm{p}^2+9n_\mathrm{p}+3)}$$

Appendix B

Let Δr and Δz be the radial and axial step lengths, respectively. Let the mesh be defined by $z_m = m\Delta z$ and $r_j = j\Delta r$. Let the numerical solution at (r_j, z_m) be defined by c_j^m. Forward marching is used in the axial direction and the radial derivatives are replaced by the following second order approximations. At all internal nodes, we use

$$c''|_j^m = \frac{c_{j+1}^m - 2c_j^m + c_{n-1}^m}{(\Delta r)^2}, \qquad c'|_j^m = \frac{c_{j+1}^m - c_{j-1}^m}{2\Delta r},$$

$$\left.\frac{\partial c}{\partial z}\right|_j^m = \frac{c_j^m - c_j^{m-1}}{\Delta z}$$

At $r = 0$ we use

$$c'|_j^m = \frac{-3c_j^m + 4c_{j+1}^m - c_{j+2}^m}{2\Delta r}$$

At $r = 1$ we use

$$c'|_j^m = \frac{3c_j^m - 4c_{j-1}^m + c_{j-2}^m}{2\Delta r}$$

Using these approximations in Eq. (13), we obtain a system of $(J-1)(L+1)$ algebraic equations for solution at each axial location. This system is block tridiagonal, in which each block is also tridiagonal. The subdiagonal, diagonal and superdiagonal entries (tridiagonal matrices of order $J-1$) are defined by $[B_2, \dots, B_{L+1}]$, $[A_1, \dots, A_{L+1}]$ and $[C_1, \dots, C_L]$, respectively. The right hand side of the system of equations is denoted by $[b_1, b_2, \dots, b_{L+1}]$ where each b_i is a column vector of order $J-1$. The solution of this system can be obtained using a standard subroutine. However, we give the following pseudocode of the system solver.

```
• Step 1:
    (a) Decompose $A_1 = \tilde{L}_1\tilde{U}_1$. Store $\tilde{L}_1, \tilde{U}_1$.
    (b) Solve $A_1Y_1 = C_1$.
```

```
    (c) Find $A_2 = A_2 - B_2 Y_1$.
    (d) Solve $A_1 z_1 = b_1$.
    (e) Modify $b_2 = b_2 - B_2 z_1$.
• Step 2:
    For $i = 2, 3, \dots, L$ do
    (a) Decompose $A_i = \tilde{L}_i \tilde{U}_i$. Store $\tilde{L}_i, \tilde{U}_i$.
    (b) Solve $A_i Y_i = C_i$.
    (c) Find $A_{i+1} = A_{i+1} - B_{i+1} Y_i$.
    (d) Solve $A_i z_i = b_i$.
    (e) Modify $b_{i+1} = b_{i+1} - B_{i+1} z_i$.
    end do.
• Step 3:
    Decompose $A_{L+1} = \tilde{L}_{L+1} \tilde{U}_{L+1}$. Store $\tilde{L}_{L+1}, \tilde{U}_{L+1}$.
    Now, the resulting matrix system is upper triangular and can be solved by back substitution.
• Step 4:
    (a) Solve $\tilde{L}_{L+1} \tilde{U}_{L+1} d_{L+1} = b_{L+1}$.
    (b) For $i = L, \dots, 1$ do
    $d_i = z_i - Y_i d_{i+1}$.end do.
```

For $m > 1$, the stored decompositions are used, as the elements of the coefficient matrices are constant.

References

[1] S. Agrawal, G. Jayaraman, Numerical simulation of dispersion in the flow of power law fluids in curved tubes, Appl. Math. Model 18 (1994) 504–512.

[2] V. Balasubramanian, G. Jayaraman, S.R.K. Iyengar, Effect of secondary flows on contaminant dispersion with weak boundary absorption, Appl. Math. Model 21 (1997) 275–285.

[3] V. Balasubramanian, G. Jayaraman, S.R.K. Iyengar, Boundary retention effects upon contaminant dispersion in secondary flows, Communicated to ZAMM, 1998.

[4] N.G. Barton, An asymptotic theory for dispersion of reactive contaminants in parallel flow, J. Aust. Math. Soc., Ser. B 25 (1984) 287–310.

[5] S.A. Berger, L. Talbot, L.S. Yao, Flow in curved pipes, Ann. Rev. Fluid Mech. 15 (1983) 461–512.

[6] T. Boddington, A.A. Clifford, The dispersion of a reactive species (atomic hydrogen) in a flowing gas, Proc. Roy. Soc. Lond. A 389 (1983) 179–196.

[7] F.A. Cleland, R.H. Wilhelm, Diffusion and reaction in viscous flow tubular reactor, AIChE J. 24 (1956) 489–497.

[8] A.A. Clifford, P. Gray, R.S. Mason, J.I. Waddicor, Measurement of the diffusion coefficients of reactive species in dilute gases, Proc. Roy. Soc. Lond. A 380 (1982) 241–258.

[9] P. Daskopoulos, A.M. Lenhoff, Flow in curved ducts: bifurcation structure for stationary ducts, J. Fluid Mech. 203 (1989) 125–148.

[10] R.H. Davis, Cross-flow microfiltration with backpulsing, in: W.K. Wang (Ed.), Membrane Separations in Biotechnology, 2nd Edition (Revised and Expanded), Marcel Dekker, New York, pp. 161–188.

[11] W.R. Dean, Note on the motion of fluid in a curved pipe, Phil. Mag. 4 (1927) 208–223.

[12] W.R. Dean, The stream line motion of fluid in a curved pipe, Phil. Mag. 5 (1928) 673–685.

[13] E.V. Evans, C.N. Kenney, Gaseous dispersion in laminar flow through a circular tube with mass transfer to a retentive layer, Proc. Roy. Soc. Lond. A 284 (1965) 562–572.

[14] W.N. Gill, M.S. Suwandi, Some aspects of isothermal laminar flow reactors, AIChE J. 9 (1963) 273–277.

[15] R.V. Homsy, R.D. Strohman, Diffusion and chemical reaction in a tubular reactor with non-Newtonian laminar flow 17 (1) (1971) 215–219.

[16] C.J. Hsu, A method of solution for mass transfer with chemical reaction under conditions of viscous flow in a tubular reactor, AIChE J. 115 (1965) 938–940.

[17] H. Ito, Flow in curved pipes (Review article), JSME Int. J. 30 (262) (1987) 543–552.

[18] M. Johnson, R.D. Kamm, Numerical studies of steady flow dispersion at low Dean number in a gently curving tube, J. Fluid Mech. 172 (1986) 329–345.

[19] G. Jayaraman, T.J. Pedley, A. Goyal, Dispersion of solute in a solvent flowing through a curved tube with absorbing walls, Q. J. Mech. Appl. Math. 51 (1998) 577–598.

[20] E.M. Lungu, H.K. Moffat, The effect of wall conductance on heat diffusion in duct flow, J. Eng. Math. 16 (1982) 121–136.

[21] R.A. Mashelkar, Applicability of axial dispersion model for non-Newtonian flow tubular reactors, Can. J. Chem. Eng. 51 (1973) 613–615.

[22] R.A. Mashelkar, C.V. Venkatasubramanian, Influence of secondary flow on diffusion with reaction, AIChE J. 313 (1985) 440–449.

[23] A. Purnama, Boundary retention effects upon contaminant dispersion in parallel flows, J. Fluid Mech. 195 (1988) 393–412.

[24] I.C. Plumb, K.R. Ryan, Method of measurement of diffusion coefficients of labile gas phase species: the diffusion coefficient of $O(^3P)$ in He at 294 K, Int. J. Chem. Kin. 15 (1983) 1081–1097.

[25] K.K. Raju, S.L. Rathna, Heat transfer for the flow of a power law fluid in a curved tube, J. Ind. Inst. Sci. 52 (1970) 34.

[26] A. Shankar, A. Lenhoff, Dispersion and partitioning in short coated tubes, Ind. Eng. Chem. Res. 30 (5) (1991) 828–835.

[27] R. Sankarasubramanian, W.N. Gill, Unsteady convective diffusion with interphase mass transfer, Proc. Roy. Soc. Lond. A 333 (1973) 115–132.

[28] R. Smith, Effects of boundary absorption upon longitudinal dispersion in shear flows, J. Fluid Mech. 134 (1983) 161–177.

[29] G.I. Taylor, Dispersion of soluble matter in a solvent flowing slowly through a tube, Proc. Roy. Soc. Lond. A 219 (1953) 186–203.